CHEMISTRY OF MATERIALS

ARTICLE

pubs.acs.org/cm

Hierarchically Porous Silica Prepared from Ionic Liquid and Polymeric Bicontinuous Microemulsion Templates

Brad H. Jones[†] and Timothy P. Lodge[*,†,‡]

[†]Department of Chemical Engineering and Materials Science and [‡]Department of Chemistry, University of Minnesota, Minneapolis, Minnesota 55455, United States

Supporting Information

ABSTRACT: Polymeric bicontinuous microemulsions (BμE) are unique disordered morphologies found in well-designed ternary blends of two immiscible homopolymers and a diblock copolymer surfactant. By crystallization or vitrification of one component and selective extraction of another, polymeric BμEs are efficient precursors to nanoporous materials having three-dimensionally continuous, ~100 nm pores. Here, nanoporous polyethylene (PE) derived from a polymeric BμE is used as a rigid template, inside which a so-called silica ionogel is synthesized. The solvent used is a room temperature ionic liquid (RTIL), and is incorporated into the silica product, yielding a disordered, bicontinuous arrangement of discrete silica and RTIL networks with ~10 nm periodicity. Because of the confinement provided by the PE template, the ionogel and PE are also arranged in a disordered, bicontinuous manner with ~100 nm periodicity. Subsequent selective extraction of the PE template by a suitable solvent generates a three-dimensionally continuous network of macropores in the ionogel. Selective extraction of the RTIL further generates a three-dimensionally continuous network of mesopores within the macropore walls. The final silica product thus contains two bicontinuous pore structures: larger macropores interconnected by smaller mesopores differing in size by over an order of magnitude. This novel, hierarchically porous material simultaneously possesses high internal surface area and a large pore framework required by advanced applications in catalysis, sensors, and purification.

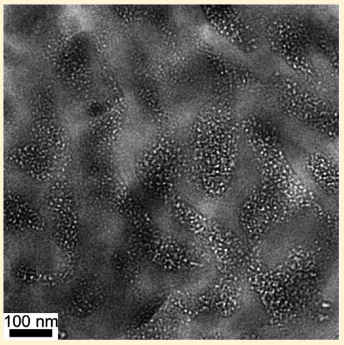

KEYWORDS: nanoporous polyethylene, bicontinuous microemulsion, hierarchically porous, macroporous, mesoporous, silica, ionic liquid, ionogel, template, nanocasting

INTRODUCTION

The development of synthetic routes to hierarchically porous materials, materials containing multiple, discrete sets of pores having disparate length scales, is a burgeoning area of research. Advanced materials for catalyst supports,[1] sensing technology,[2] and water purification,[3] among other applications, require combinations of functionalities and properties that are often most readily enabled through hierarchical arrangements of matter. For example, highly efficient membranes or particles for catalyst supports must exhibit high surface areas, so as to permit maximal catalyst loading per volume and to enhance reaction yield. Simultaneously, such materials must allow rapid mass transport to and from catalyst sites, so as to minimize the time or applied pressure necessary to obtain sufficient amounts of product. These properties can be achieved through the synthetic design of hierarchically porous materials, whereby an intervening macropore structure facilitates mass transport through the material, and the macropore framework is independently microporous or mesoporous, having short, high surface area pores.[4]

In the past decade or so, researchers have used clever combinations of soft- and hard-templating techniques to create a variety of hierarchically porous inorganic materials. Davis and co-workers provided a seminal example in 1997, using hexgonally packed filaments of *B. subtilis* as a hard template for the surfactant-directed synthesis of MCM-41 silica.[5] The calcined fiber product simultaneously exhibited mesopores and macropores, generated by the surfactant-silica self-assembly and filament template, respectively. Many of the strategies that have since been developed feature the same key pathways; namely, a microstructured or mesostructured material, templated by small molecules or by surfactant or block polymer mesophases, is casted within a hard template defined by an arrangement of comparatively large objects or a large-pore network. Colloidal particles have been used extensively to define the large pore structure, that is, the hard template.[1,6−17] For example, Yang, et al. demonstrated hierarchically porous silica and metal oxides by syntheses directed with Pluronic poly(alkyleneoxide) triblock copolymers and confined within the interstitial void space of a colloidal crystal of 200 nm diameter polystyrene spheres.[7] After removal of the copolymer and colloid templates, the products contained spherical macropores surrounded by mesoporous

Received: July 27, 2011
Revised: September 28, 2011
Published: October 11, 2011

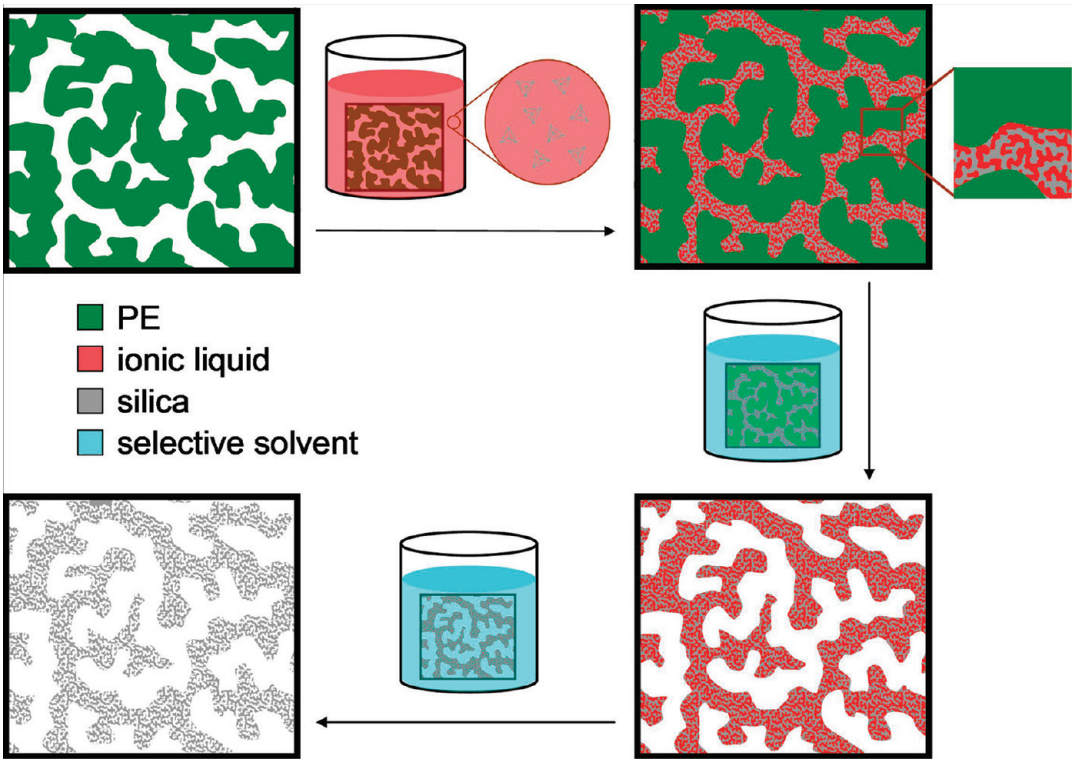

Figure 1. Templating route employed to synthesize hierarchically structured silica-organic hybrid and hierarchically porous silica materials. The pores of nanoporous PE having a BμE structure are infiltrated with a solution of silica precursor in a RTIL. Condensation of the precursor results in a mesostructured, bicontinuous silica/RTIL composite within the PE pore system. Subsequent selective solvent extraction of the PE template, followed by the RTIL, generates a bicontinuous network of macropores having silica pore walls that contain a bicontinuous network of mesopores. Note that the pores of the PE template are, in fact, coated with a thin layer of PEP[54] that is not shown for simplicity.

frameworks of hexagonal or cubic (bicontinuous) symmetry. The diameters of the spherical cavities produced by colloidal crystal templates can be readily tuned across essentially the entire mesopore and macropore ranges, simply through the choice of template particle size. However, the cavities are typically interconnected by smaller pore windows, corresponding to the points of contact or closest proximity between neighboring particles. Hence, the large pore frameworks comprising these hierarchically porous materials, while bicontinuous, have nonuniform overall pore size and shape, and their mass transport properties may ultimately be dictated by the smaller interconnecting pores. Alternative hard templates that have been successfully used to prepare hierarchically porous materials include eggshell-derived membranes,[18,19] wood tissue,[20] polyurethane foams,[21−23] cellulose acetate and other filtration membranes,[24,25] starch gels,[26] polyacrylamide-based hydrogels,[27,28] agarose gels,[29] carbon black aggregates,[30] and aerogels.[31,32] Because of the inherent structures of the templates, the larger pores in these materials generally possess ambiguous or nonuniform pore shapes and sizes.

Hierarchically porous inorganic materials have also been prepared without the use of hard templates. Instead, self-assembly and phase separation processes occurring over disparate length scales are simultaneously exploited to generate hierarchical precursor structures.[33−50] Generally, a precursor to a mesostructured material is diluted with a significant amount of an incompatible small molecule or polymer. Macroscopic phase separation between two phases, composed primarily of the precursor mixture and the diluent, proceeds concurrently with conversion of the former. This phase separation can be arrested by gelation (i.e., in the sol−gel condensation of an inorganic network) or other means. For example, Zhao and co-workers added Pluronic poly(alkyleneoxide) triblock copolymers and inorganic salts to silica sols in ethanol.[35] The resultant copolymer-structured silica and electrolyte medium exhibited phase separation by spinodal decomposition. Subsequent removal of the copolymer, salts, and solvent yielded a material with a disordered, bicontinuous network of macropores of which the pore walls contained hexagonally packed, cylindrical mesopores. The spinodal decomposition mechanism that is typically used to generate large pores in these processes results in fairly uniform pore shapes and sizes. In addition, the pore size is usually tunable over a wide range by controlling the amount of diluent added, as well as the separation kinetics. However, the minimum macropore size that has been demonstrated in these materials is on the order of hundreds of nanometers.

The approach to hierarchically porous silica described herein is inspired by and complementary to these previous efforts. A new hard template is utilized to impart a macropore network into mesoporous silica, derived from a polymeric BμE. Polymeric BμEs are equilibrium, disordered melt phases, found universally in ternary blends of two immiscible homopolymers A and B and their corresponding A-B diblock copolymer.[51,52] They consist of interpenetrating networks of A and B with vanishing interfacial tension, near-zero mean interfacial curvature, and periodicity on the order of 100 nm. Previously, we have demonstrated that nanoporous PE can be obtained from a PE/poly(ethylene-*alt*-propylene) (PEP) BμE by crystallization of the former and selective solvent extraction of the latter.[53,54] In addition, we have

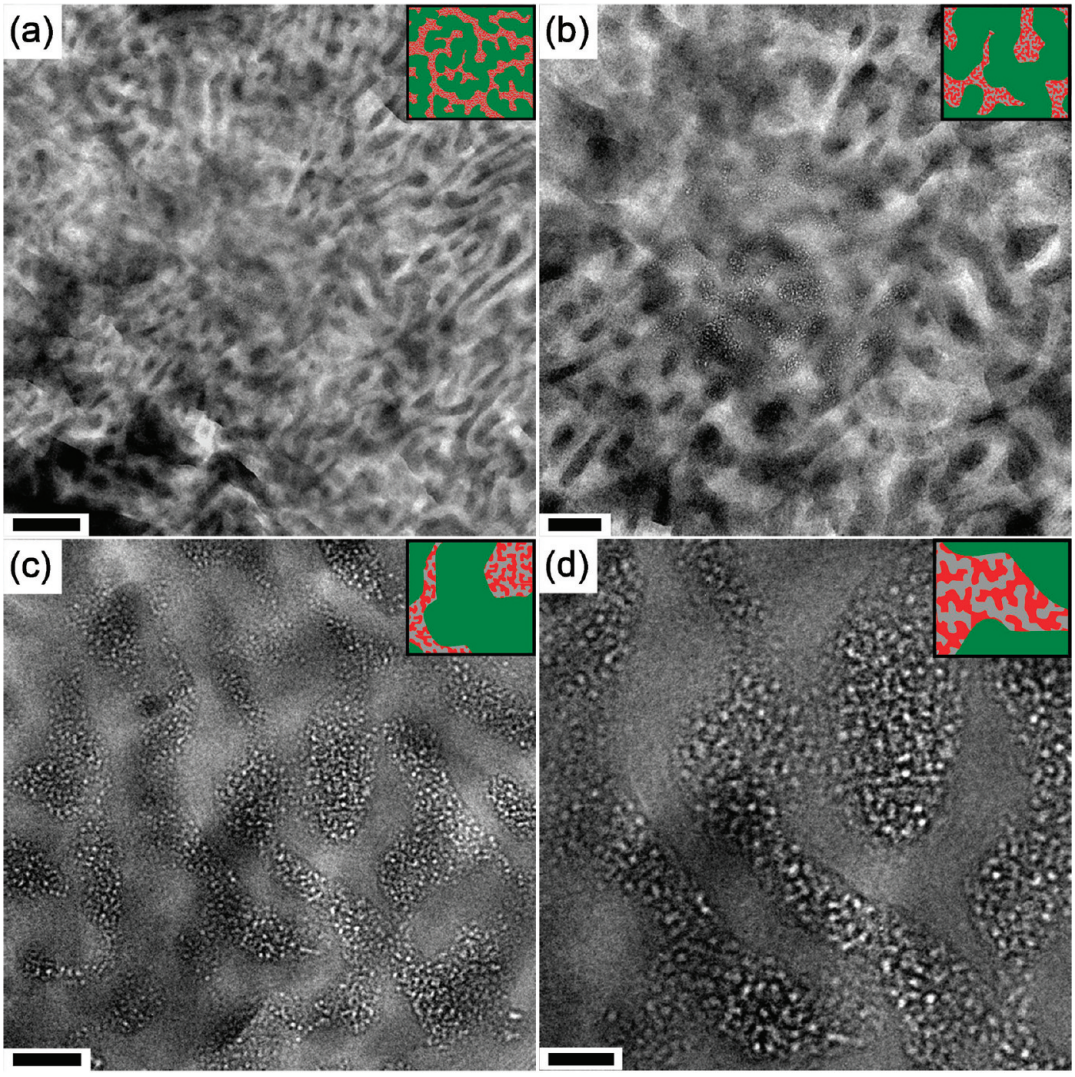

Figure 2. TEM images of hierarchically structured monolith obtained from confined synthesis of silica in [BMIM][BF_4] solvent within nanoporous PE. The magnification increases monotonically from (a) through (d). The material is unstained; contrast derives from the electron density differences between PE, silica, and [BMIM][BF_4] and may be enhanced by beam damage. Each inset shows a cartoon depiction of the structure seen in the corresponding TEM image; the PE, silica, and [BMIM][BF_4] domains are represented in green, gray, and red, respectively. Scale bars indicate (a) 500, (b) 200, (c) 100, and (d) 50 nm.

shown that this nanoporous PE can be used as a hard template in the synthesis of robust, single-phase materials, such as ceramics and thermosets. These materials have three-dimensionally continuous pore networks that replicate the original BμE structure with high precision. The pores are of uniform shape and size, centered at ~100 nm and predictable from scattering of radiation by the original BμE. At present, we extend our approach to the production of hierarchically porous materials through the synthesis of mesostructured silica within the same nanoporous PE template. A schematic representation of the pathway employed is shown in Figure 1. A nonaqueous sol−gel synthesis of silica is conducted, confined within nanoporous PE, using the RTIL 1-butyl-3-methylimidazolium tetrafluoroborate, [BMIM][BF_4], as a solvent. This unique solvent and synthesis route, first demonstrated by Zhou, Schattka, and Antonietti, provides a disordered, bicontinuous, distribution of inorganic- and RTIL-rich domains with mesoscale periodicity, because of the molecular stacking of the solvent ions and the hydrogen bonds it forms with the condensing silica network.[55] At present, this so-called ionogel is localized within one domain of the BμE structure imposed by the hard PE template. Selective solvent extraction of the PE, followed by the RTIL, generates macropores and then mesopores within the macropore walls, respectively. The resulting silica material is doubly bicontinuous and possesses two discrete, but interconnected, uniformly sized pore networks, differing in pore size by over an order of magnitude.

EXPERIMENTAL METHODS

Nanoporous PE monoliths were derived from polyolefin BμEs, composed of PE (M_n = 23 kg/mol, M_w/M_n = 1.05), PEP (M_n = 23 kg/mol, M_w/M_n = 1.02), and poly(ethylene-*b*-ethylene-*alt*-propylene) (PE-PEP, M_n = 101 kg/mol, M_w/M_n = 1.07), as described previously.[53,54] Briefly, PE, PEP, and PE-PEP were blended at volume fractions of 0.425, 0.425, and 0.15, respectively, by dissolution in benzene at 70 °C, followed by freeze-drying. The blend was heated to 132 °C and held for 2 h to allow the development of a BμE morphology,

dx.doi.org/10.1021/cm202170g |*Chem. Mater.* 2011, 23, 4824–4831

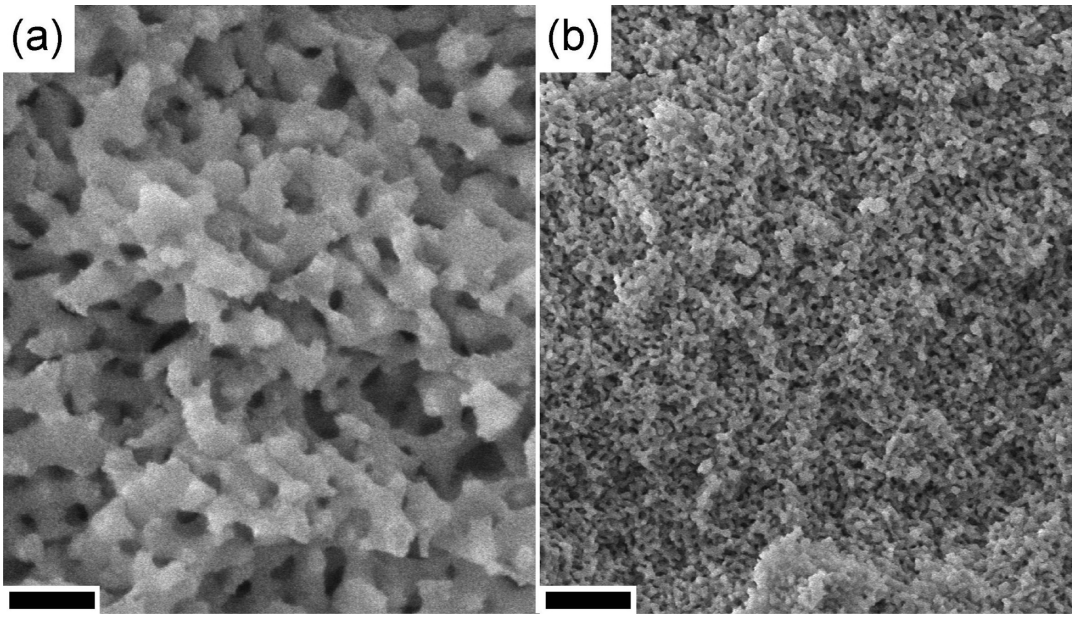

Figure 3. (a) High and (b) low magnification SEM images of hierarchically porous silica obtained after selective extraction of PE template and [BMIM][BF_4] solvent from hierarchically structured PE-silica-[BMIM][BF_4] composite. The bicontinuous macropore network imprinted by the BμE structure of the PE template persists across large areas. The mesopores within the macropore walls are not visible at these magnifications. Scale bars indicate (a) 300 nm and (b) 1.5 μm.

after which the PE domains were crystallized by quenching in liquid nitrogen. Finally, nanoporous PE was obtained by selective extraction of the PEP homopolymer with tetrahydrofuran.

A silica ionogel was synthesized within nanoporous PE following a slightly modified procedure from that reported previously.[55] [BMIM][BF_4] was synthesized according to the procedure described in a recent publication.[56] Typically, a prescribed amount of [BMIM][BF_4] was mixed with an excess of dichloromethane under stirring (>3:1 CH_2Cl_2:-[BMIM][BF_4] by vol.). A nanoporous PE monolith was added to this mixture and allowed to rest for at least one hour. With the PE monolith still present, the dichloromethane was removed from the mixture under nitrogen flow and then vacuum. This sequence is required to infiltrate [BMIM][BF_4] into the PE pores; separate experiments indicated that pure [BMIM][BF_4] is not spontaneously imbibed by the nanoporous PE, but a solution of [BMIM][BF_4] in dichloromethane is. Tetramethylorthosilicate (TMOS, 99+%, Aldrich) was then added to the [BMIM][BF_4] in a 5:6 volume ratio of TMOS:[BMIM][BF_4] under vigorous stirring. Zhou, et al. previously reported homogenization of this mixture;[55] however, in this case, a single phase mixture was never observed, even after stirring for several hours at different temperatures. This may be due to differing purities of the respective [BMIM][BF_4] used, for instance, due to incomplete anion exchange from a [BMIM][Cl] precursor.[56] Nevertheless, the hydrolysis of TMOS was next catalyzed by the addition of 0.01 M aqueous HCl at a 1:2 volume ratio of HCl solution/TMOS. The total stirred mixture completely homogenized within several seconds after this addition and was subsequently stirred for ~2 h. The mixture was then exposed to vacuum at room temperature, followed by heating to 60 °C. This removes the methanol byproduct from the hydrolysis of TMOS, driving the condensation of silanol species into a silica network. The mixture solidified within ~1 to 2 h under vacuum and was then allowed to stand in air at 60 °C for 48 h. The resulting product consisted of a PE monolith embedded in a larger transparent monolith of silica. The silica monolith was split to extract the PE monolith, and excess silica was cleaned from the surface by mechanical abrasion. The PE monolith, containing a mesostructured ionogel within its pore network, was soaked in toluene at 72 °C to selectively extract and void the PE domains. Finally, the composite was soaked in acetonitrile at 90 °C to selectively extract and void the [BMIM][BF_4] domains. The product obtained after each selective extraction was dried under vacuum.

Transmission electron microscopy (TEM) was performed using a FEI Tecnai G^2 F30 field emission gun instrument, operated at 300 kV accelerating voltage. Images were obtained with an Ultrascan 4000 by 4000 pixel charge coupled device camera. The analyzed samples consisted of two different forms. The hierarchically structured PE/ionogel composite was cut into ~85−200 nm sections at −100 °C using a Leica UC6 cryogenic ultramicrotome. These sections were then dispersed onto an uncoated copper mesh grid. Hierarchically porous silica was substantially brittle and, as such, was ground into a fine powder with a ceramic mortar and pestle. This powder was then dispersed onto a carbon coated copper mesh grid. Small angle X-ray scattering (SAXS) measurements were performed using a custom built line equipped with a Rigaku rotating anode source (λ = 0.1542 nm) and a Bruker area detector. The sample-to-detector distance was 2.47 m. Samples were sandwiched between two pieces of Kapton film separated by a Viton O-ring and patterns were collected at room temperature. The isotropic two-dimensional scattering patterns obtained were azimuthally integrated to afford one-dimensional patterns of scattered intensity versus wavevector q. Scanning electron microscopy (SEM) was performed using a Hitachi S-900 microscope, operated at voltages ranging from 2 to 5 kV. Fracture surfaces were created by grinding samples with a ceramic mortar and pestle. These fracture surfaces were mounted on metal stubs via conductive carbon tape and coated with thin layers of Pt using a VCR indirect ion-beam sputtering system. Nitrogen sorption measurements were conducted at 77 K using a Quantachrome Instruments Autosorb iQ. Samples were degassed at 120 °C overnight prior to measurement.

RESULTS AND DISCUSSION

The hierarchically structured material that is obtained from the [BMIM][BF_4]-based condensation of TMOS confined within BμE-derived nanoporous PE is shown in Figure 2. The low

dx.doi.org/10.1021/cm202170g |*Chem. Mater.* 2011, 23, 4824–4831

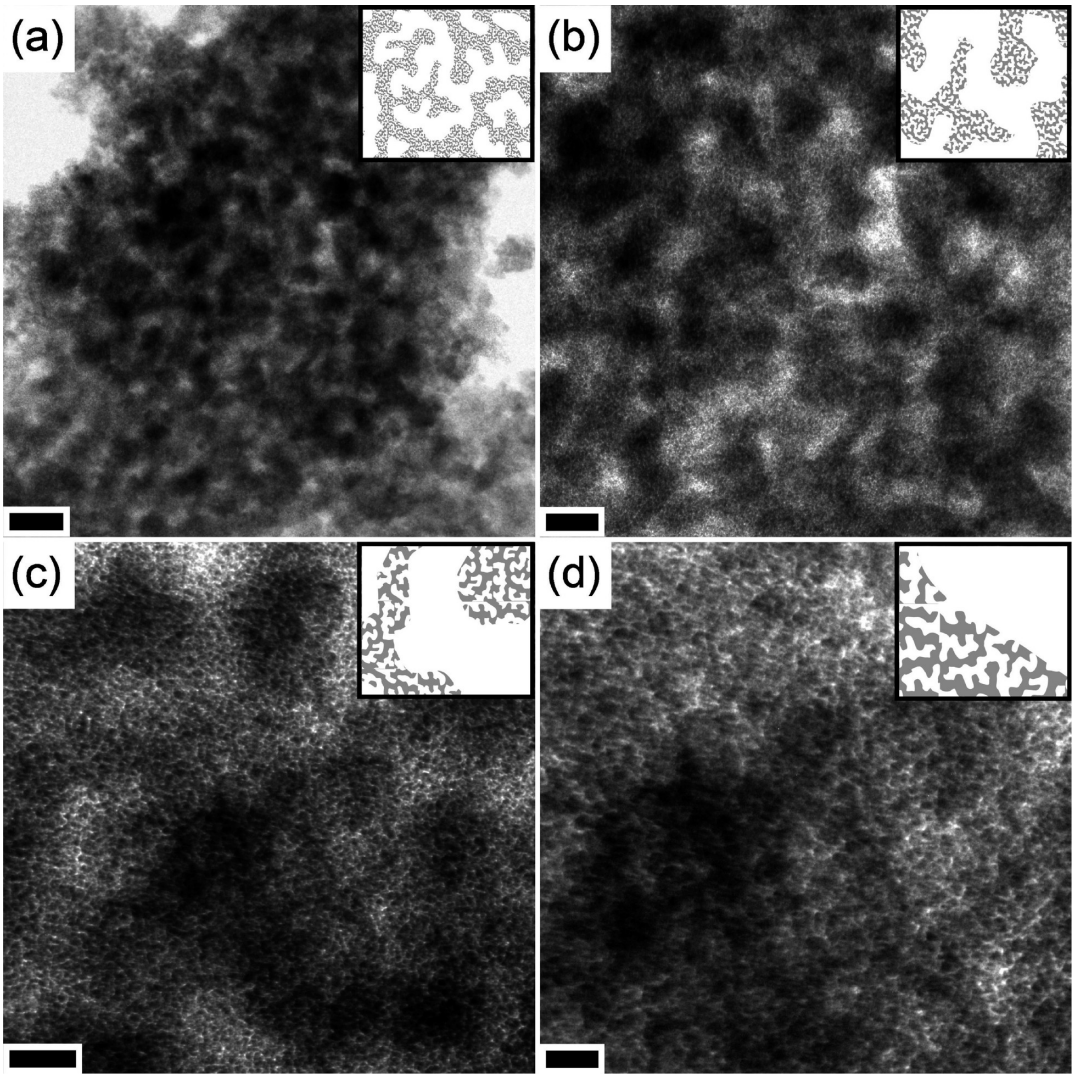

Figure 4. TEM images of hierarchically porous silica. The magnification increases monotonically from a through d. All contrast derives from the electron density difference between silica and vacuum (pores). Each inset shows a cartoon depiction of the structure seen in the corresponding TEM image; the silica domains and pores are represented in gray and white, respectively. Scale bars indicate (a) 200, (b) 100, (c) 50, and (d) 20 nm.

magnification images in parts a and b clearly demonstrate that the BμE structure of the PE template is imprinted into the nanocast material. Distinct bright and dark, disordered, interpenetrating networks are observed, with periodicity on the order of 100 nm. The electron densities of silica and [BMIM][BF_4] are both greater than PE, so the bright and dark domains of the BμE structure correspond to PE and the confined ionogel, respectively. At high magnification (parts c and d), the mesoscale segregation of silica and [BMIM][BF_4] within the latter domains is apparent. The inorganic and ionic liquid phases exhibit a disordered, bicontinuous arrangement of wormlike domains, mimicking the BμE structure imposed by the PE template, but with periodicity on the order of 10 nm. Zhou, Schattka, and Antonietti, who first reported the synthetic route to mesostructured silica employed, postulated that self-assembly of the condensing silica network and the [BMIM][BF_4] is mediated by hydrogen bonding and intramolecular interactions involving the unique RTIL solvent.[55] Silanol groups formed from the hydrolysis of TMOS hydrogen bond with the [BF_4] anion, inducing local coordination between the inorganic framework and the ionic liquid. The [BMIM] cations further arrange into an extended molecular conformation, driven by $\pi-\pi$ interactions between neighboring imidazolium rings that favor stacking of the cations parallel to the long axis of the wormlike domains. The domain sizes of the mesostructured composite are thus linked to the molecular size of [BMIM][BF_4].

With regard to Figure 2, the electron density of the amorphous silica phase is expected to be greater than that of the [BMIM][BF_4] and, as such, the silica is assumed to appear darkest in these images. It was also discovered that the contrast between silica and [BMIM][BF_4] was enhanced as the sample was continually exposed to the electron beam. This can be seen in part b, where the segregation between silica and [BMIM][BF_4] within the darker domains of the BμE is faintly visible, but only in the middle portion of the image. This portion had previously been irradiated with a high flux of electrons to obtain the relatively high magnification images in parts c and d. The observance of this phenomenon implies that beam damage of the specimen plays at least some role in the generation of contrast between the silica and [BMIM][BF_4] domains. Such considerations

notwithstanding, the images unequivocally show that a unique polymer-ceramic-ionic liquid composite, containing two bicontinuous networks with distinct length scales, is obtained through a straightforward, one-pot synthesis confined within a BμE-derived template.

The PE and [BMIM][BF_4] domains of the hierarchically structured material are easily voided by selective solvation. After treatment in hot toluene, a good solvent for PE, a mass loss is observed within 10% of the mass of the original nanoporous PE monolith, consistent with quantitative removal of the PE template. After further treatment in hot acetonitrile, a good solvent for [BMIM][BF_4], the product mass decreases by an additional 79%. Indeed, after accounting for the conversion of TMOS to SiO_2, the [BMIM][BF_4] is calculated to comprise 78% by mass of the ionogel, hence this mass loss is consistent with quantitative removal of the [BMIM][BF_4]. In Figure 3, SEM images of the porous material resulting from these successive solvent treatments are provided. The images reveal a macroporous material containing a three-dimensionally continuous, disordered, ~100 nm pore network. The pore structure of the BμE-derived PE template is successfully imprinted into silica by nanocasting, yielding a qualitatively identical replica of the template. Moreover, as seen in Figure 3b, this pore structure extends over large areas of the sample. The anticipated mesoporous structure comprising the macropore walls, however, could not be observed with SEM. Due to the insulating character of silica and the high degree of porosity, deposition of relatively thick Pt coatings (>2 nm) on the material's surfaces was necessary to render them sufficiently conductive. This fact, coupled with the several nm resolution limit of the SEM used, obscured any structural detail existing within the macropore walls.

On the other hand, TEM was used to simultaneously observe the existence of both the macropore and mesopore networks in hierarchically porous silica. A series of representative TEM images is presented in Figure 4. At low magnification (parts a and b), the BμE-templated macropore network is again visible as a result of the electron density contrast between silica (dark) and pores (bright). At higher magnification (parts c and d), the mesoporous structure existing within the macropore walls becomes apparent. Part d, in particular, demonstrates that the anticipated three-dimensionally continuous network of wormlike mesopores is obtained from voiding of the self-assembled [BMIM][BF_4] domains. Although a quantitative estimate of the mesopore size from these images is delicate, the pores do appear to be uniform in size with diameters of several nm. Indeed, SAXS measurements (Supporting Information, Figure S1) indicate a characteristic periodicity of ~14 nm, consistent with this general observation. Figure 4c is an especially striking illustration of the disparately sized pore networks contained in this single material, as both bicontinuous networks are discernible. The image size is simultaneously equivalent to several and several hundred times the periodicity of the BμE- and RTIL-templated pore structures, respectively, underscoring the fact that the corresponding pore sizes differ by over an order of magnitude. It is important to note that the apparent existence of mesopores within the bright regions defining the macropore network is simply an illusion, created from the projection of the three-dimensional volume sampled by the electron beam into a two-dimensional image.

To provide a quantitative estimate of the pore characteristics exhibited by hierarchically porous silica, nitrogen sorption experiments were carried out. Figure 5 shows the adsorption and

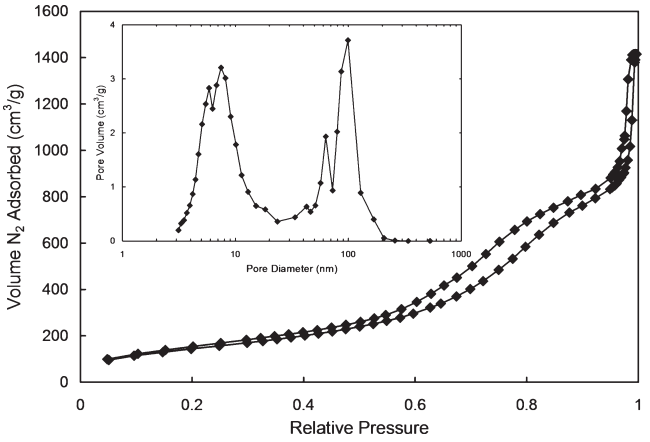

Figure 5. Nitrogen adsorption/desorption isotherm of hierarchically porous silica. The hysteresis loops are associated with capillary condensation/evaporation of N_2 in the mesopore and macropore networks of the material. The inset shows the pore size distribution of the material, plotted as the cumulative pore volume versus pore diameter, calculated from the desorption branch of the isotherm.

desorption isotherm, as well as the pore size distribution calculated from the desorption branch according to the method of Barrett, Joyner, and Halenda.[57] The hysteresis loop of the isotherm reflects the general pore characteristics seen by TEM, in that pores of two distinct sizes are evident. More specifically, the nearly vertical step at relative pressures very close to unity is indicative of capillary condensation and evaporation of N_2 in the BμE-templated macropore network, while the step occurring at relative pressures ranging from ~0.6 to 0.8 is indicative of the same phenomenon in the RTIL-templated mesopore network. The latter feature is consistent with the previously reported isotherm of [BMIM][BF_4]-templated, mesoporous silica.[55] Importantly, the existence of this feature implies that the mesopores residing within the internal macropore walls are accessible from the surface of the material and, hence, the entire hierarchical pore system is interconnected. The internal surface area presented by the pores is 570 m^2/g, calculated by the method of Brunauer, Emmett, and Teller.[58] This value, coupled with the macropore structure seen in Figure 3, suggest that the hierarchically structured silica is an excellent candidate for applications requiring materials having both high surface areas and low mass transport barriers.

The calculated pore size distribution provides quantitative evidence of the hierarchical arrangement of pores within the silica material. Two distinct peaks are unambiguously observed, centered at pore sizes of approximately 6−7 nm and 90−100 nm. The latter peak is similar to that found previously after nanocasting of homogeneous, single-phase materials using the same BμE-derived PE template.[53,54] As mentioned previously, the former peak is consistent with the characteristic periodicity of ~14 nm determined from SAXS measurements (Supporting Information, Figure S1). This average mesopore size is 2 to 3 times larger than the ~2.5 nm diameter initially reported by Zhou, Schattka, and Antonietti.[55] It is important to note that their assignment was made on the basis of TEM images, rather than nitrogen isotherms. The potential discrepancy between the mesopore structures obtained at present and in the previous work could be caused by several factors. As noted in the experimental details, there is reason to suspect that the [BMIM][BF_4] used may differ

in purity, the present version having been synthesized by anion exchange from [BMIM][Cl]. Furthermore, the measurement of the appropriate amount of reagents used in the ionogel synthesis was done volumetrically, implying inherently low precision. Indeed, the pore sizes obtained in the synthesis of silica templated by 1-butyl-3-methylimidazolium bis(trifluoromethylsulfonyl)amide, or [BMIM][TFSA], were found to be quite sensitive to the amount of RTIL solvent used, with increased concentrations resulting in larger mesopores with broader size distributions.[59] Presumably, the mesopore size obtained in the present material could be tuned similarly by adjusting the composition of the reaction mixture infiltrated into the PE template. Even further, the local mesostructure of the infiltrated reaction mixture may be affected by the confining presence of the hydrophobic PE template. Preferential interactions between the condensing silica network, the RTIL, and the pore wall may induce specific segregation states of the components in the vicinity of the wall-mixture interface, which could, in turn, perturb the local arrangement of components toward the interior of the domain.

CONCLUSIONS

In summary, BμE-derived nanoporous PE has been used as a template in the creation of novel hierarchically structured materials by a simple nanocasting route. The sol−gel synthesis of silica, using the RTIL [BMIM][BF_4] as a unique solvent, confined within the three-dimensionally continuous pore network of the PE template directly affords a material with arrangements of matter at both ∼100 nm and ∼10 nm scales. The product material exhibited a BμE-like arrangement of discrete PE and ionogel networks; within the latter, an additional disordered, bicontinuous arrangement of silica and RTIL was clearly present. The periodicity defining these two bicontinuous arrangements differed by over an order of magnitude. Straightforward exposure of the material to selective solvents for the PE template and RTIL was used to void the corresponding domains. The final product is, thus, hierarchically porous and doubly bicontinuous, having a three-dimensionally continuous network of uniform macropores, wherein the pore walls are comprised of a three-dimensionally network of uniform mesopores. The former should enable rapid mass transport of fluids through the pore system, while the latter confers high surface area to the material. The simultaneous demonstration of these properties in a single porous material is a prerequisite for advanced materials in catalysis, sensors, and purification. Because of its uniform pore sizes and highly interconnected pore systems, this hierarchically porous silica is a potentially outstanding candidate for such applications.

ASSOCIATED CONTENT

Supporting Information. SAXS patterns and additional discussion. This information is available free of charge via the Internet at http://pubs.acs.org.

AUTHOR INFORMATION

Corresponding Author
*E-mail: lodge@umn.edu.

ACKNOWLEDGMENT

This work was supported by the MRSEC program of the National Science Foundation under Award No. DMR-0819885. Portions of this work were carried out using instrumentation provided by the University of Minnesota Characterization Facility. We gratefully acknowledge Lucas McIntosh for performing SAXS measurements and Dr. Hau-Nan Lee for synthesizing and providing the [BMIM][BF_4]. We also acknowledge Dr. Adam Moughton for helpful discussion.

REFERENCES

(1) Yuan, Z.-Y.; Su, B.-L. *J. Mater. Chem.* **2006**, *16*, 663–677.
(2) Zhang, J.; Wang, S.; Xu, M.; Wang, Y.; Zhu, B.; Zhang, S.; Huang, W.; Wu, S. *Cryst. Growth Des.* **2009**, *9*, 3532–3537.
(3) Hu, J.-S.; Zhong, L.-S.; Song, W.-G.; Wan, L.-J. *Adv. Mater.* **2008**, *20*, 2977–2982.
(4) Micro, meso, and macro denote sizes <2 nm, 2−50 nm, or >50 nm, respectively, according to the accepted definitions set by the International Union of Pure and Applied Chemistry: Sing, K. S. W.; Everett, D. H.; Haul, R. A. W.; Moscou, L.; Pierotti, R. A.; Rouquérol, J.; Siemieniewska, T. *Pure Appl. Chem.* **1985**, *57*, 603–619.
(5) Davis, S. A.; Burkett, S. L.; Mendelson, N. H.; Mann, S. *Nature* **1997**, *385*, 420–423.
(6) Antonietti, M.; Berton, B.; Göltner, C.; Hentze, H.-P. *Adv. Mater.* **1998**, *10*, 154–159.
(7) Yang, P.; Deng, T.; Zhao, D.; Feng, P.; Pine, D.; Chmelka, B. F.; Whitesides, G. M.; Stucky, G. D. *Science* **1998**, *282*, 2244–2246.
(8) Holland, B. T.; Abrams, L.; Stein, A. *J. Am. Chem. Soc.* **1999**, *121*, 4308–4309.
(9) Yin, J. S.; Wang, Z. L. *Appl. Phys. Lett.* **1999**, *74*, 2629–2631.
(10) Huang, L.; Wang, Z.; Sun, J.; Miao, L.; Li, Q.; Yan, Y.; Zhao, D. *J. Am. Chem. Soc.* **2000**, *122*, 3530–3531.
(11) Dong, A.; Wang, Y.; Tang, Y.; Zhang, Y.; Ren, N.; Gao, Z. *Adv. Mater.* **2002**, *14*, 1506–1510.
(12) Sen, T.; Tiddy, G. J. T.; Casci, J. L.; Anderson, M. W. *Angew. Chem., Int. Ed.* **2003**, *42*, 4649–4653.
(13) Zhou, Y.; Antonietti, M. *Chem. Commun.* **2003**, 2564–2565.
(14) Kuang, D.; Brezesinski, T.; Smarsly, B. *J. Am. Chem. Soc.* **2004**, *126*, 10534–10535.
(15) Fan, W.; Snyder, M. A.; Kumar, S.; Lee, P.-S.; Yoo, W. C.; McCormick, A. V.; Penn, R. L.; Stein, A.; Tsapatsis, M. *Nat. Mater.* **2008**, *7*, 984–991.
(16) Zhang, S.; Chen, L.; Zhou, S.; Zhao, D.; Wu, L. *Chem. Mater.* **2010**, *22*, 3433–3440.
(17) Zhao, B.; Collinson, M. M. *Chem. Mater.* **2010**, *22*, 4312–4319.
(18) Yang, D.; Qi, L.; Ma, J. *Adv. Mater.* **2002**, *14*, 1543–1546.
(19) Yang, D.; Qi, L.; Ma, J. *J. Mater. Chem.* **2003**, *13*, 1119–1123.
(20) Shin, Y.; Liu, J.; Chang, J. H.; Nie, Z.; Exarhos, G. J. *Adv. Mater.* **2001**, *13*, 728–732.
(21) Lee, Y.-J.; Lee, J. S.; Park, Y. S.; Yoon, K. B. *Adv. Mater.* **2001**, *13*, 1259–1263.
(22) Lee, Y.-J.; Yoon, K. B. *Microporous Mesoporous Mater.* **2006**, *88*, 176–186.
(23) Li, L.-L.; Duan, W.-T.; Yuan, Q.; Li, Z.-X.; Duan, H.-H.; Yan, C.-H. *Chem. Commun.* **2009**, 6174–6176.
(24) Wang, Y.; Tang, Y.; Dong, A.; Wang, X.; Ren, N.; Shan, W.; Gao, Z. *Adv. Mater.* **2002**, *14*, 994–997.
(25) Drisko, G. L.; Cao, L.; Kimling, M. C.; Harrisson, S.; Luca, V.; Caruso, R. A. *ACS Appl. Mater. Interf.* **2009**, *1*, 2893–2901.
(26) Zhang, B.; Davis, S. A.; Mann, S. *Chem. Mater.* **2002**, *14*, 1369–1375.
(27) Wang, H.; Huang, L.; Wang, Z.; Mitra, A.; Yan, Y. *Chem. Commun.* **2001**, 1364–1365.
(28) Liang, C.; Dai, S.; Guiochon, G. *Chem. Commun.* **2002**, 2680–2681.
(29) Drisko, G. L.; Luca, V.; Sizgek, E.; Scales, N.; Caruso, R. A. *Langmuir* **2009**, *25*, 5286–5293.
(30) Jacobsen, C. J. H.; Madsen, C.; Houzvicka, J.; Schmidt, I.; Carlsson, A. *J. Am. Chem. Soc.* **2000**, *122*, 7116–7117.

(31) Tao, Y.; Kanoh, H.; Kaneko, K. *J. Am. Chem. Soc.* **2003**, *125*, 6044–6045.
(32) Li, W.-C.; Lu, A.-H.; Palkovits, R.; Schmidt, W.; Spliethoff, B.; Schüth, F. *J. Am. Chem. Soc.* **2005**, *127*, 12595–12600.
(33) Minakuchi, H.; Nakanishi, K.; Soga, N.; Ishizuka, N.; Tanaka, N. *Anal. Chem.* **1996**, *68*, 3498–3501.
(34) Nakanishi, K. *J. Porous Mater.* **1997**, *4*, 67–112.
(35) Zhao, D.; Yang, P.; Chmelka, B. F.; Stucky, G. D. *Chem. Mater.* **1999**, *11*, 1174–1178.
(36) Nakanishi, K.; Takahashi, R.; Nagakane, T.; Kitayama, K.; Koheiya, N.; Shikata, H.; Soga, N. *J. Sol−Gel Sci. Technol.* **2000**, *17*, 191–210.
(37) Nakamura, N.; Takahashi, R.; Sato, S.; Sodesawa, T.; Yoshida, S. *Phys. Chem. Chem. Phys.* **2000**, *2*, 4983–4990.
(38) Smått, J.-H.; Schunk, S.; Lindén, M. *Chem. Mater.* **2003**, *15*, 2354–2361.
(39) Lu, A.-H.; Smått, J.-H.; Backlund, S.; Lindén, M. *Microporous Mesoporous Mater.* **2004**, *72*, 59–65.
(40) Brandhuber, D.; Torma, V.; Raab, C.; Peterlik, H.; Kulak, A.; Hüsing, N. *Chem. Mater.* **2005**, *17*, 4262–4271.
(41) Smått, J.-H.; Weidenthaler, C.; Rosenholm, J. B.; Lindén, M. *Chem. Mater.* **2006**, *18*, 1443–1450.
(42) Konishi, J.; Fujita, K.; Nakanishi, K.; Hirao, K. *Chem. Mater.* **2006**, *18*, 864–866.
(43) Konishi, J.; Fujita, K.; Nakanishi, K.; Hirao, K. *Chem. Mater.* **2006**, *18*, 6069–6074.
(44) Wang, H.; Pinnavaia, T. J. *Adv. Mater.* **2006**, *45*, 7603–7606.
(45) Sakatani, Y.; Boissière, C.; Grosso, D.; Nicole, L.; Soler-Illia, G. J. A. A.; Sanchez, C. *Chem. Mater.* **2008**, *20*, 1049–1056.
(46) Huang, Y.; Cai, H.; Feng, D.; Gu, D.; Deng, Y.; Tu, B.; Wang, H.; Webley, P. A.; Zhao, D. *Chem. Commun.* **2008**, 2641–2643.
(47) Hasegawa, G.; Kanamori, K.; Nakanishi, K.; Hanada, T. *J. Am. Ceram. Soc.* **2010**, *93*, 3110–3115.
(48) Drisko, G. L.; Zelcer, A.; Luca, V.; Caruso, R. A.; Soler-Illia, G. J.; de, A. A. *Chem. Mater.* **2010**, *22*, 4379–4385.
(49) Lee, M. N.; Mohraz, A. *Adv. Mater.* **2010**, *22*, 4836–4841.
(50) Lee, M. N.; Mohraz, A. *J. Am. Chem. Soc.* **2011**, *133*, 6945–6947.
(51) Bates, F. S.; Maurer, W. W.; Lipic, P. M.; Hillmyer, M. A.; Almdal, K.; Mortensen, K.; Fredrickson, G. H.; Lodge, T. P. *Phys. Rev. Lett.* **1997**, *79*, 849–852.
(52) Hillmyer, M. A.; Maurer, W. W.; Lodge, T. P.; Bates, F. S.; Almdal, K. *J. Phys. Chem. B* **1999**, *103*, 4814–4824.
(53) Jones, B. H.; Lodge, T. P. *J. Am. Chem. Soc.* **2009**, *131*, 1676–1677.
(54) Jones, B. H.; Lodge, T. P. *Chem. Mater.* **2010**, *22*, 1279–1281.
(55) Zhou, Y.; Schattka, J. H.; Antonietti, M. *Nano Lett.* **2004**, *4*, 477–481.
(56) Lee, H.-L.; Lodge, T. P. *J. Phys. Chem. Lett.* **2010**, *1*, 1962–1966.
(57) Barrett, E. P.; Joyner, L. G.; Halenda, P. P. *J. Am. Chem. Soc.* **1951**, *73*, 373–380.
(58) Brunauer, S.; Emmett, P. H.; Teller, E. *J. Am. Chem. Soc.* **1938**, *60*, 309–319.
(59) Néouze, M.-A.; Bideau, J. L.; Gaveau, P.; Bellayer, S.; Vioux, A. *Chem. Mater.* **2006**, *18*, 3931–3936.